ELSEVIER

Engineering Analysis with Boundary Elements 32 (2008) 770–777

ENGINEERING ANALYSIS with BOUNDARY ELEMENTS

www.elsevier.com/locate/enganabound

A complex parameter boundary element method for modeling AC impedances of electrochemical systems by analytic continuation—Application to a slit geometry

Bosco Emmanuel

Modeling and Simulation Group, Central Electrochemical Research Institute, Karaikudi 630006, India

Received 9 May 2007; accepted 13 November 2007
Available online 3 January 2008

Abstract

A complex parameter boundary element method is advanced to compute the AC impedances of electrochemical systems by solving the Laplace equation with complex boundary conditions. This method, which is based on analytic continuation from the corresponding secondary current distribution, is applied to a slit geometry, besides two illustrative cases: plane-parallel electrodes and concentric cylinder electrodes. The AC impedance responses for the slit geometry are computed for several electrode and slit dimensions for (1) purely capacitive working electrode and (2) a working electrode represented by a Voigt element. Interesting effects of the electrode and the slit dimensions on the AC response are noted. Applications of this method in viscoelastic systems, rheology and electronic/electrical devices are discussed. User-friendly implementations of the method in the BEASY group of softwares are also suggested.

Keywords: Boundary element method; Analytic continuation; AC impedance; Transmission line models; Complex boundary conditions; Slit geometry; Electrochemical systems

1. Introduction

The boundary element method (BEM), a cousin of the finite element method (FEM), has demonstrated its utility in several areas of science and engineering since its inception by Brebbia [1,2]. It is also not new to electrochemistry or electrochemical engineering. In particular, it has been used to compute the current–potential distributions for a host of cathodic protection problems (see Ref. [3] and articles cited therein), including an application by the present author to the cathodic protection of complex off-shore structures in the Arabian Sea [4]. BEASY has developed several softwares in this area and our research group has contributed one to the Oil and Natural Gas Corporation of India. Besides corrosion, electro-deposition, electrochemical machining and electroforming are three other important areas where the current–potential distribution is the central problem to solve in electrochemistry. In all electrochemical systems the seat of action is at the electrode boundaries and hence BEM is ideally suited. In a typical current–potential distribution problem, we solve the Laplace equation with Dirichlet, Neumann or Robin boundary conditions. In addition to the current–potential distributions corresponding to any stationary state of the system, one is very often interested in the response of the electrochemical system when perturbed by a small amplitude AC signal. This response is measured in terms of a complex impedance function, in contrast to the stationary current–potential distribution, which are real functions. AC impedance spectroscopy, the name by which this area is known, provides a versatile experimental tool to probe the interfacial electrode processes, diagnose their mechanisms and estimate the underlying kinetic parameters in a wide group of electrochemical systems [5]. In this paper we describe a method of computing the AC impedances of electrochemical systems with arbitrary geometries using a complex extension of the BEM. Besides electrochemistry, this complex parameter BEM will be useful in several related areas, such as solid-state and dielectric devices and

E-mail address: boscoemmanuel@yahoo.co.in

0955-7997/$ - see front matter © 2007 Elsevier Ltd. All rights reserved.
doi:10.1016/j.enganabound.2007.11.004

elastic media whenever a linear system is perturbed by a sinusoidal input signal [be it electrical (current/potential), mechanical (stress/strain) or electromagnetic (incident radiation in spectroscopy)] and the system responds by producing a phase-shifted signal superposed on the input signal. A complex extension of the BEM is required to model the frequency-dependent AC response in all these cases. The author learns from an anonymous reviewer that problems with complex boundary conditions have been solved with the BEM in acoustics and fluid flow. However the present application to electrochemical systems is completely new and is expected to be widely useful for the BEM-based computation of electrochemical AC impedances; in fact, it establishes a benchmark for evaluating the results of existing approximate theories based on the transmission line model (TLM).

When electrochemists solve the impedance problem on non-trivial geometries, such as the cylindrical pore and the saw-tooth geometry, they usually invoke the TLM [6,7] with some physical/geometric approximation for the model parameters. The TLM is an interesting model pioneered by de Levie. It has an intuitive appeal and has been subjected to good and extensive use by electrochemists. Even fractal electrode surfaces have been modeled using the TLM, besides a host of simpler geometries [8–11]. However, the limitations of the TLM are well known [5]. We recently advanced a method [12] to compute the exact AC impedance of electrochemical systems having arbitrary geometry, without recourse to the TLM. More specifically, given a system and its current distribution, say as a solution of the Laplace equation with appropriate boundary conditions, we deduced the AC response of the system solely from the solution to the current distribution problem by applying analytic continuation either to the exact solution or to a numerical solution method.

The purpose of this article is to introduce this method to the practitioners of the BEM, though in an electrochemical setting. Section 2 introduces the electrochemical system and its concepts and terms needed for this paper. In Section 3, the method of analytic continuation is briefly sketched and illustrated, for its pedagogical value, with the help of two otherwise most trivial problems: that of 1-D and concentric cylinder electrodes. For non-trivial geometries, no analytic solution is of course available for the secondary current distribution from which to obtain the AC impedance by analytic continuation. Hence it was found necessary to incorporate the "analytic continuation" in the numerical solution method itself. This is done in Section 4 within the frame work of the BEM. Essentially, we use a complex extension of the BEM. Applications of this method to an electrochemical system wherein the space between the electrodes has a single-slit constriction for the current lines are in Section 5. Section 6 has summary and concluding remarks.

The complex extension of the BEM used in this paper should be clearly distinguished from the complex variable BEM developed by Hromadka and Lai [13], wherein BEM is reformulated using complex spatial variables, whereas the complexity enters through the parameters in the present work. For the same reason our method does not have any dimensional restrictions. Hence our method may be appropriately named complex-parameter BEM.

2. The electrochemical system

An electrochemical system has a minimum of two electrodes, a working electrode (WE) where the electrochemical reaction/process of interest takes place and a counter-electrode (CE) to complete the current circuit. The CE is usually so chosen that it offers negligible resistance to the current flow, in which case the system response will essentially be independent of the reaction/process at the CE. However there are also situations where both the electrodes will together determine the system response. When the experimenter controls the potential (current) between the two electrodes, the system responds by setting up an appropriate current (potential) distribution in the system which is measured. Several processes, such as double-layer charging, electron transfer at the electrode/electrolyte interface, and charge and mass transport in the electrolyte together determine this response. When the charge transport in the electrolyte alone is important the response is called primary current distribution that depends only on the system geometry. Secondary current distributions result if the interfacial processes (double-layer charging and electron transfer) also contribute. Tertiary current distributions include mass transport.

To be specific, consider the secondary current-distribution problem (sketched in Fig. 1) involving an electrolyte medium of conductivity κ enclosed between two electrode boundaries B1 and B2. The differential equation to be solved for the potential distribution ϕ with variable conductivity is

$$\nabla(\kappa\nabla\phi) = 0, \tag{1}$$

which reduces to the standard Laplace equation

$$\nabla^2\phi = 0, \tag{2}$$

when κ is uniform in space. Eqs. (1) or (2) describe the charge transport in the electrolyte. The interfacial processes, double-layer charging and electron transfer enter through the boundary conditions. However, double-layer charging will not contribute to a secondary current distribution in the steady state. Hence, for the steady state,

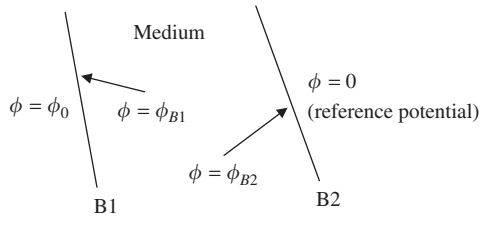

Fig. 1. A two-electrode system, defining the different potentials. B1 is the working electrode and B2 the counter-electrode.

a typical boundary condition, say at the boundary B1, will be

$$\text{at B1}, \quad \kappa \nabla \phi = \frac{\phi_{\mathrm{B1}} - \phi_0}{R_{ct,1}}, \tag{3}$$

where $R_{ct,1}$ is the electron-transfer resistance (usually known as charge-transfer resistance) at the electrode/electrolyte interface at B1. In general the RHS of Eq. (3) can be a non-linear function of ϕ_{B1}–ϕ_0. As we are interested in relating the current distribution to the small signal AC response, this linear relation (termed linear polarization by electrochemists) should suffice; ϕ_0 and ϕ_{B1} are, respectively, the potentials at the electrode side and electrolyte side of the electrode boundary B1, which may be taken as the WE. In general a similar condition may be applied at B2. However, for the purposes of this present work and without loss of generality, we take B2 as a CE with zero charge transfer resistance (i.e. a perfectly leaky capacitor) and consequently its role is restricted to its geometrical influence on the current distribution. By the same token, this leaky capacitor cannot hold any charge and hence does not affect the AC response either. We set $\phi_{\mathrm{B2}} = 0$. However, we must keep in mind that for systems where both the electrodes influence the response, as for example in an electrorefining cell, one will have to maintain boundary conditions similar to Eq. (3) at both the electrodes.

3. AC response and the method of analytic continuation

For modeling the AC response of our system perturbed by a time-dependent AC signal, the double-layer charging which was left out should also be included in the boundary condition Eq. (3), which now becomes

$$\text{at B1}, \quad \kappa \nabla \phi = \frac{\phi_{\mathrm{B1}} - \phi_0}{R_{ct,1}} + C_{dl} \frac{\partial(\phi_{\mathrm{B1}} - \phi_0)}{\partial t}. \tag{3'}$$

In the frequency domain in which the AC impedance is defined, this requires the replacement of $R_{ct,1}$ in Eq. (3) by $(1/R_{ct,1} + \mathrm{j}\omega C_{dl})^{-1}$. We shall call this Z_1. C_{dl} is the double-layer capacitance, ω the frequency of the AC signal and $\mathrm{j} = \sqrt{-1}$. Thus the steady-state response and the AC response of our system is connected by an analytic continuation. If $\phi(x, y, z; \kappa\ R_{ct,1}$, etc.) is the exact (or approximate) solution to the Laplace equation (2) with boundary conditions such as Eq. (3), the analytic continuation consists in replacing the real charge-transfer resistance $R_{ct,1}$ by its complex extension Z_1.

It may be further noted that, in conventional electrochemical systems, the medium conductivity κ is usually taken as real (i.e. purely resistive). However, κ is known to be complex for some media (the reader may consult the recent book by Barsoukov and Macdonald [5] for several examples); solid media, with grains and grain boundaries, are an important class, where κ is complex. In such cases, we must of course do the analytic continuation in κ also, besides $R_{ct,1}$. Essentially, one takes a real current–potential distribution and analytically continues it to obtain the complex current–potential distribution having the phase information at each point of the 3D space. In the simplest case the complexity enters through the boundary conditions and in the general case it may enter through the complex response of the medium also.

The above prescription for analytically continuing the DC current–potential distribution is also easily established by discretising the medium and the boundaries into discrete volume and surface elements and applying Kirchoff's law to the resulting network. (This network is an exact analogue of the physical system and is no way connected with the TLM. Nor does it involve the use of any lumped model parameters which the TLM does.) Such an analysis leads to the following expression for the AC admittance of the system:

$$Y = \frac{\int_{\mathrm{B1}} \kappa \nabla \phi \, \mathrm{d\,B1}}{\phi_0} \tag{4}$$

where ϕ is the analytical continuation of the potential distribution and hence is now complex. Note further that, interestingly, ϕ_0 in Fig. 1 turns out to be the amplitude of the applied AC signal. The potential distribution ϕ used in this paper is reckoned from the unperturbed initial state which may be an equilibrium or a steady state.

Two simple illustrations of the method are given below.

3.1. The case of 1-D

This case corresponds to two large planar electrodes kept parallel to one another at a distance of L:

$$\frac{\partial^2 \phi}{\partial x^2} = 0, \tag{5}$$

$$-\kappa \frac{\partial \phi}{\partial x} = \frac{\phi_0 - \phi}{R_{ct,1}} \quad \text{at } x = 0, \tag{6}$$

$$-\kappa \frac{\partial \phi}{\partial x} = \frac{\phi}{R_{ct,2}} \quad \text{at } x = L. \tag{7}$$

This system is trivially solved to obtain the potential and current distribution:

$$\phi = \phi_0 + \phi_0 \frac{(x + \kappa R_{ct,1})}{(\kappa R_{ct,1} + \kappa R_{ct,2} + L)}, \tag{8}$$

$$-\kappa \nabla \phi|_{\mathrm{B1}} = i = -\frac{\phi_0}{R_{ct,1} + R_{ct,2} + (L/\kappa)}, \tag{9}$$

where i is the current density. Replacing in Eqs. (8) and (9), $R_{ct,1}$ and $R_{ct,2}$ by Z_1 and Z_2, the corresponding interfacial impedances, we obtain the complex potential and current. Now, the admittance follows from Eqs. (4) and (9) as

$$Y = \frac{A}{Z_1 + Z_2 + (L/\kappa)}, \tag{10}$$

the expected result. A is the area of the electrode, $Z_1 = (1/R_{ct,1} + \mathrm{j}\omega\ C_{dl,1})^{-1}$ and Z_2 is similarly defined.

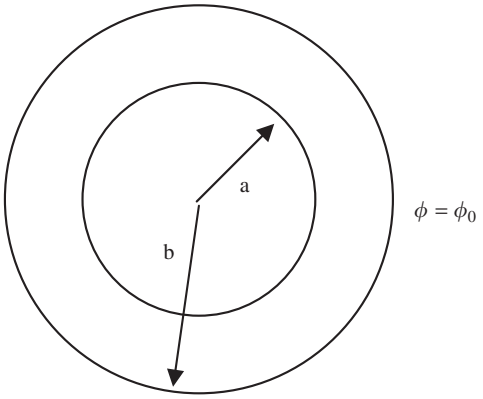

Fig. 2. Two concentric cylinder electrodes, of radii a and b, and with the outer electrode kept at potential ϕ_0 with respect to the inner electrode.

3.2. Concentric cylinder electrodes

This case corresponds to the concentric cylinder electrodes shown in Fig. 2:

$$\frac{\partial^2\phi}{\partial r^2} + \frac{1}{r}\frac{\partial\phi}{\partial r} = 0, \tag{11}$$

$$-\kappa\frac{\partial\phi}{\partial r}|_{r=b} = \frac{\phi(b)-\phi_0}{R_{ct,b}}, \tag{12}$$

$$\phi(a) = 0. \tag{13}$$

Solving this system, we obtain the following potential and current distribution:

$$\phi(r) = \frac{\phi_0}{\{\ln(b/a) + (\kappa/b)R_{ct,b}\}}\ln\left(\frac{r}{a}\right), \tag{14}$$

$$i = -\kappa\frac{\phi_0}{r\{\ln(b/a) + (\kappa/b)R_{ct,b}\}}. \tag{15}$$

The analytic continuation $R_{ct,b}\to Z_b$ gives the complex potential and current distributions. The system admittance is

$$Y = \frac{A}{\{Z_b + (b/\kappa)\ln(b/a)\}}, \tag{16}$$

where A is the area and $Z_b = (1/R_{ct,b} + j\omega C_{dl,b})^{-1}$ the interfacial impedance of the outer electrode.

4. The boundary element method and analytic continuation

As discussed in Sections 2 and 3, the primary and the secondary current distributions should be clearly distinguished at the outset. The former depends only on the system geometry and the electrolyte conductivity, the latter depends in addition on the two interfacial processes: electron transfer and the electrical double-layer charging. Further, primary current distributions are governed by Dirichlet's or Neumann's boundary conditions and the secondary current distributions employ the Robin's boundary condition (see Eqs. (3) and (3′)). Hence, for primary current distributions, any complexity can enter the description only through a complex electrolyte conductivity κ, in which case the corresponding AC admittance, given as

$$Y = \kappa\frac{\int_{B1}\nabla\phi\,\mathrm{d}\,B1}{\phi_0}, \tag{4′}$$

is trivially complex through the complex multiplicative factor κ. However, for the frequency range of interest to electrochemical systems, κ is essentially real and the AC admittance (or impedance) is purely resistive. On the other hand, for secondary current distributions, the complexity enters through the Robin's boundary condition (Eq. (3′)) in an essential and non-trivial way. In the frequency domain, Eq. (3′) transforms to

$$\text{at B1,}\quad \kappa\nabla\phi = \frac{\phi_{B1}-\phi_0}{R_{ct,1}} + j\omega C_{dl}(\phi_{B1}-\phi_0), \tag{3″}$$

where the potentials ϕ and ϕ_{B1}–ϕ_0 now represent the frequency-dependent transforms of the original time-dependent potentials. Clearly Eq. (3″) can be viewed as resulting from Eq. (3) when $R_{ct,1}$ in Eq. (3) is replaced by $(1/R_{ct,1} + j\omega C_{dl})^{-1}$. It is this interesting observation which makes it possible to obtain the complex AC response as an analytic continuation of the DC response (i.e. the secondary current distribution).

Turning now to the question of implementing this analytic continuation, this is merely a direct substitution of a real by a complex quantity in the case of exactly solvable models as illustrated in Section 3. While the primary current distribution problem has been solved for many 2D geometries using conformal transformations, neither exact nor approximate solutions are available for secondary current distributions in non-trivial geometries even in 2D. Hence we need to resort to numerical implementation of the analytic continuation.

In this section we adopt the BEM for the numerical solution and embed analytic continuation. Essentially, it is a complex extension of the BEM. The mathematical details of the BEM, pioneered by Brebbia [1,2], are well documented in the literature to which we refer the interested reader [1,2,14]. Omitting the mathematical details, we describe only the final equations of BEM relevant for our present context. The simultaneous equations to which the BEM eventually reduces is the following:

$$\sum_{j=1}^{N} L_{ij}P_j - \sum_{j=1}^{N} H_{ij}\phi_j = 0 \tag{17}$$

with i running form 1 to N, the number of boundary elements, ϕ_j and P_j are, respectively, the potential and the normal gradient of the potential (related to the current $I_j = -\kappa P_j$) at the jth boundary element. L_{ij} and H_{ij} are the boundary element integrals which incorporate the Green's function of the PDE (the Laplace equation in our case) and also the system boundary information. The boundary conditions are not yet included. Typically we encounter, in

the present work, any one of the following three types of boundary conditions on the jth element:

$$\text{Dirichlet's condition}: \quad \phi_j = \text{a given value}, \tag{18}$$

$$\text{Neuman's condition}: \quad P_j = \text{a given value} = 0 \text{ for insulating boundary elements}, \tag{19}$$

$$\text{Robin's condition}: \quad P_j = -\frac{1}{\kappa R_{ct}}(\phi_j - \phi_0), \tag{20}$$

for boundary elements subject to linear polarization.

Now we perform analytic continuation by replacing R_{ct} (in the Robin's boundary condition) by the interfacial impedance Z_1. The AC admittance of the system follows easily as

$$Y = \left(\sum_j I_j\right) \Big/ \phi_0, \tag{21}$$

where I_j is the complex current normal to the jth boundary element and the summation runs over the boundary elements on the WE (or on the CE; the equality of the two,[1] in the real and imaginary parts separately, provides a good check on the whole complex calculation).

5. Application to electrochemical cells with slit geometries

In a previous work [12] we studied the AC response of several electrochemical cells like the Hull cells, the rectangular and saw-tooth cells and the fractal electrode. Detailed comparisons with the TLMs showed that the TLM could go wrong, both qualitatively and quantitatively. The present exact method based on analytic continuation will be the only option for cell geometries where one may not be able to formulate a TLM.

In this section we apply the method outlined in the previous section to slit cell geometries (Fig. 3) and compute the Nyquist plots for a purely capacitive WE (Figs. 4(a)–(e)) and for a WE with a charge-transfer resistance in parallel to the double layer capacitance, i.e. a Voigt element (Figs. 5(a)–(d)). The distance between the counter and the WE, the width of the slit and the length of the CE are fixed at convenient values, while the height of the slit and the length of the WE are varied. For constructing the Nyquist plots the real and imaginary parts of the impedance (the reciprocal of the admittance in Eq. (4)) was computed for several frequencies in the range 1 Hz–1 GHz. The double layer, the charge transfer and the conductivity parameters are given for each plot. For the purely capacitive WE, Fig. 4(b) shows the expected vertical line while, in Figs. 4(a) and (c), there is an interesting tilt of the Nyquist plot from the vertical line. This difference can be attributed to the fact that the length of the WE was set equal to the length of the CE for computing Fig. 4(b), whereas the length of the WE was smaller than that of the CE for computing Figs. 4(a) and (c). Thus the AC response of the slit cell is able to sense the dimension of the WE. Smaller the WE, larger is the tilt! This is not the complete story. When we probe closely the high-frequency region [kHz–MHz] of these plots, as in Fig. 4(d), we notice an interesting frequency dispersion with clearly defined effective electrolyte resistances for the high and low frequency limits: the intercept on the real axis and the position of the vertical asymptote, respectively. However, for the conventional rectangular cell, there is virtually no frequency dependence of the real part of the impedance, with the high and low frequency limits of the effective electrolyte resistance coinciding (see Fig. 4(e)). Hence, for the rectangular geometry alone, this electrolyte resistance is given by the simple formula

$$R = l/\kappa a,$$

where l is the length and a the area of cross-section of the rectangular cell. For any other geometry, we need to compute the high and low frequency limits of this resistance by solving the Laplace equation in the complex domain, as is done in this paper. Figs. 5(a)–(d) show that the AC response of the slit cell when the WE is represented by a Voigt element. Such Nyquist plots have important information on the electrochemical system. For example, the first intercept on the real axis gives the effective solution resistance in the high-frequency limit, while the second intercept (measured from the first) gives the charge-transfer resistance at the electrode–elctrolyte interface. Note that when the slit height increases from 0.2 to 5 cm, the effective solution resistance decreases from ~80 to ~24 Ω (see Figs. 5(a)–(c)). Further, the solution resistance depends on the length of the WE too: it is ~24 Ω for a WE 1 cm long and ~20 Ω for a WE 5 cm long. Besides the effective solution resistance, the length of the WE affects the effective charge-transfer resistance also. For a WE 1 cm

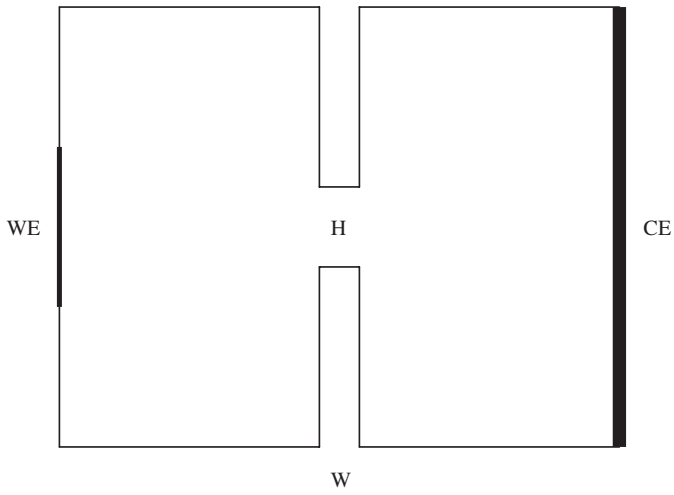

Fig. 3. The slit geometry showing the working electrode (WE), the counter-electrode (CE), the slit height H and the slit width W. The thinner line is the insulating boundary of the cell.

[1] Except for the sign, which should be different.

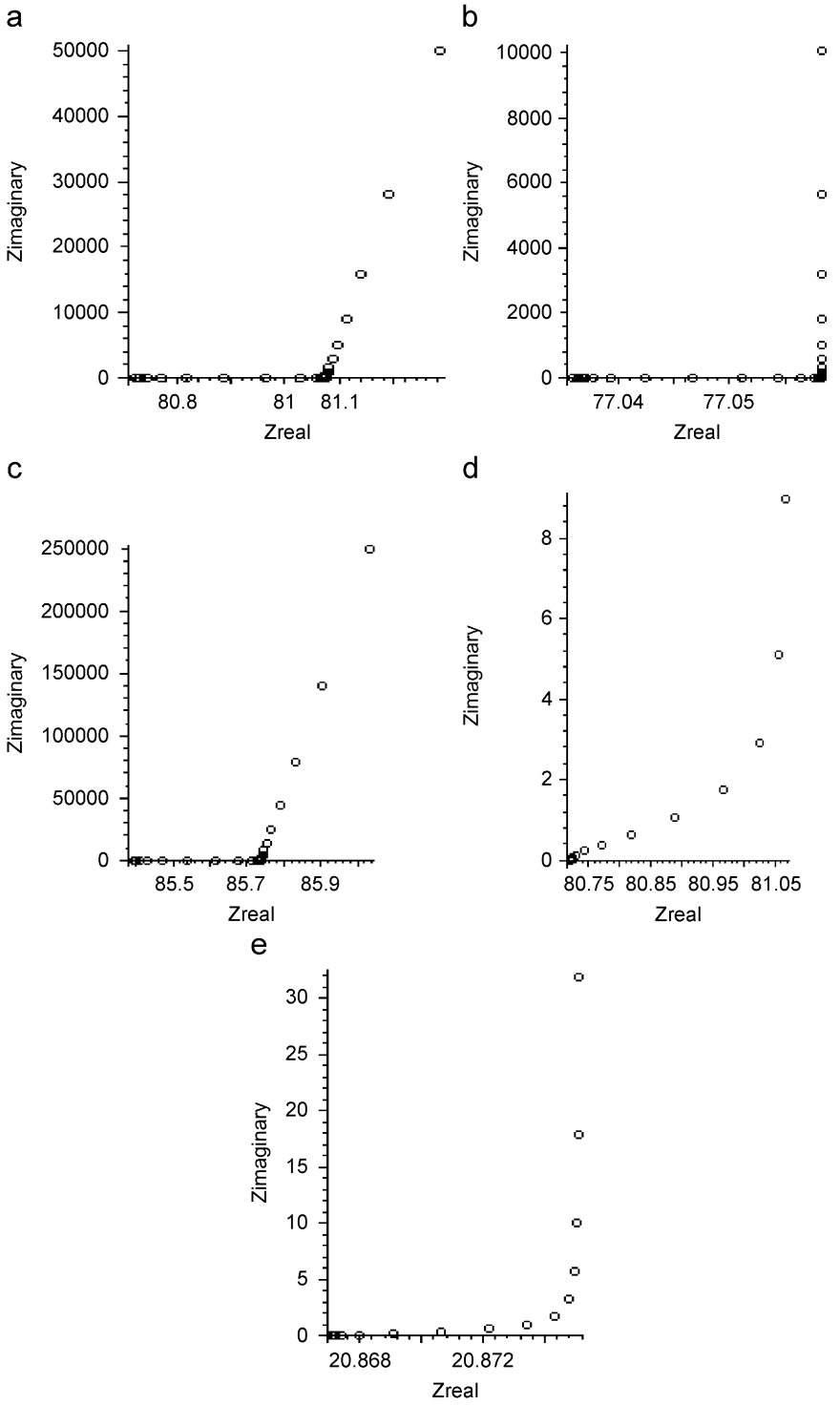

Fig. 4. Nyquist plots for the AC response of the slit cell with a purely capacitive working electrode of dimensions: (a) WE 1 cm, H 0.2 cm, (b) WE 5 cm, H 0.2 cm, (c) WE 0.2 cm, H 0.2 cm, (d) WE 1 cm, H 0.2 cm (range: kHz–MHz) and (e) WE 5 cm, H 5 cm (range: kHz–MHz).

long the effective charge-transfer resistance is $\sim 250\,\Omega$ and it is $\sim 50\,\Omega$ for a 5 cm long WE (see Figs. 5(c) and (d)). Fig. 5(d) is the classical semi-circle for the rectangular cell geometry.

Needless to say, a great practical advantage of our present method is that it computes, at one strike, the current distribution, effective solution resistances and the AC impedance of electrochemical systems of arbitrary geometry.

6. Summary and concluding remarks

A method, based on a simple and elegant analytic continuation from the secondary current distribution, was

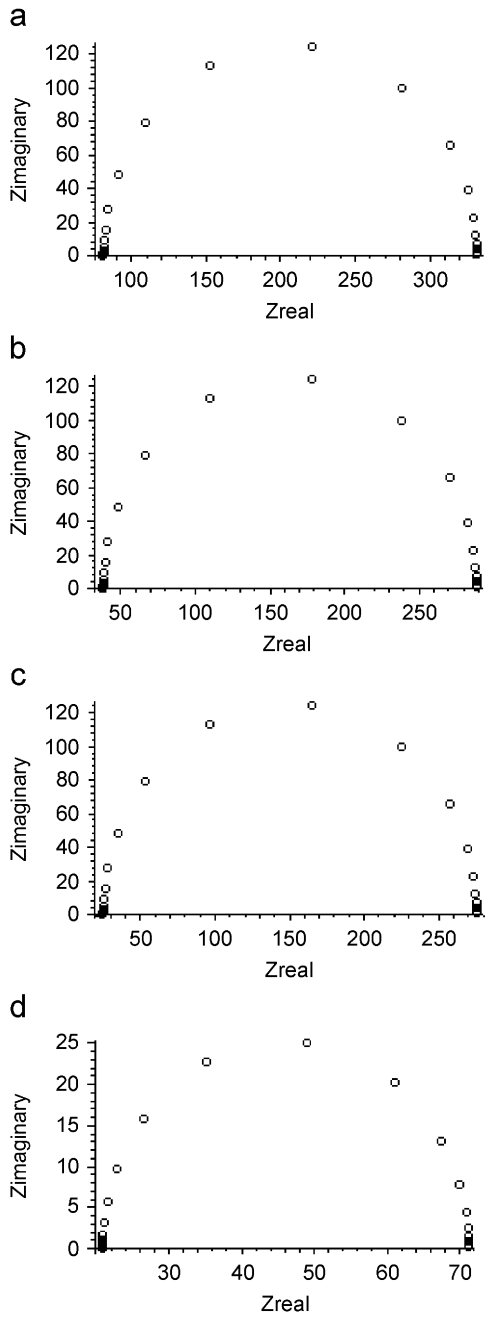

Fig. 5. Nyquist plots for the AC response of the slit cell with a Voigt-type working electrode of dimensions: (a) WE 1.0 cm, H 0.2 cm (real-axis-intercepts: ~80 and ~331 Ω), (b) WE 1.0 cm, H 1.0 cm (real-axis intercepts: ~37 and ~288 Ω), (c) WE 1.0 cm, H 5.0 cm (real-axis-intercepts: ~24 and ~275 Ω) and (d) WE 5.0 cm, H 5.0 cm (real-axis-intercepts: ~20.86 and ~71.27 Ω).

applied to model the AC response of an electrochemical system with a slit geometry. Several cell dimensions were investigated and the Nyquist response was shown to be very sensitive to the dimensions of the WE and the slit. Cells with double slits were also studied and qualitatively similar predictions were obtained. This work also establishes the BEM as the most convenient method to embed analytic continuation in the solution of the Laplace equation for the current–potential distribution problem. It can also be made user friendly by implementing it in BEM-based softwares such as BEASY. Though FEMLAB also has been used [15] to numerically compute the AC response of a thin-film rectangular geometry, we believe that, for electrochemical systems where processes at the interfacial boundaries need to be understood, the BEM is a better choice.

The complex extension of the BEM which we have used opens up the possibility of computing the AC responses for any complicated geometry. It also provides a good benchmark for evaluating the predictions of approximate theories based on the TLMs. Though we restricted ourselves, in the use of BEM, to two dimensions and secondary current distributions, the method presented is more general. Extensions to three dimensions and tertiary current distributions are well within its ambit.

The method of analytic continuation reported in this paper for the modeling of AC responses of arbitrary electrode geometries is not restricted to electrochemical systems. For example, in rheology and in other viscoelastic systems [16], the mechanical stress and strain play the role of the potential and the current and Hooke's law is the mechanical analogue of the Ohm's law. For complex mechanical systems, such as the liquid crystals, the Hooke's law may not be adequate to describe the stress–strain relationship; reactive components which are the mechanical analogues of capacitors and inductors will be needed. The strain may now lead or lag behind the stress and the viscoelastic response will become complex. Our method will prove useful for all such systems. Besides, for a host of electronic/electrical devices with non-trivial medium and electrode geometries, the AC response can be similarly computed.

Acknowledgements

The author thanks an anonymous reviewer for comments and suggestions which improved the manuscript.

References

[1] Brebbia CA. The boundary element method for engineers. New York: Wiley; 1978.
[2] Brebbia CA, Telles JCF, Wrobel LC. Boundary element techniques, theory and applications in engineering. Berlin, Heidelberg: Springer; 1984.
[3] Ramanan VS, Muthukumar M, Gnanasekaran S, Venkataramana Reddy MJ, Emmanuel B. Green's functions for the Laplace equation in a 3-layer medium, boundary element integrals, and their application to cathodic protection. Eng Anal Boundary Elements 1999;23:777–86.
[4] CPSAE++: a software for cathodic protection modeling of offshore structures. SW-1153/2003.
[5] Barsoukov E, Macdonald JR. Impedance spectroscopy (theory, experiment and applications). 2nd ed. New Jersey: Wiley-Interscience; 2005 [Chapter 2].
[6] de Levie R. Electrochemical response of porous and rough electrodes. In: Delahay P, editor. Advances in electrochemistry and electrochemical engineering, vol. 6. New York: Wiley; 1967.

[7] de Levie R. The influence of surface roughness of solid electrodes on electrochemical measurements. Electrochim Acta 1965;10: 113–30.
[8] Liu SH. Fractal model for the AC response of a rough interface. Phys Rev Lett 1985;55(5):529–32.
[9] Scheider W. Theory of the frequency dispersion of electrode polarisation: topology of networks with fractional power frequency dependence. J Phys Chem 1975;79(2):127–36.
[10] Keiser H, Beccu KD, Gutjahr MA. Abschatzung der porenstruktur poroser elektroden aus impedanzmessungen. Electrochim Acta 1976;21:539–43.
[11] Macdonald DD. Reflections on the history of electrochemical impedance spectroscopy. Electrochim Acta 2006;51:1376–88.
[12] Emmanuel B. J Electroanal Chem 2007;605:89–97.
[13] Hromadka II TV, Lai C. The complex variable boundary element method in engineering analysis. Berlin: Springer; 1987.
[14] Ramachandran PA. Boundary element methods in transport phenomena. London: Elsevier; 1994.
[15] Adler SB. Reference electrode placement in thin solid electrolytes. J Electrochem Soc 2002;149:E166–72.
[16] Christensen RM. Theory of viscoelasticity: an introduction. New York: Academic Press; 1982.